Spectrum emitted by hot electrons in *p-i-n* cold cathodes

Kees de Kort, Paul Damink, and Henk Boots
Philips Research Laboratories, P.O. Box 80.000, 5600 JA Eindhoven, The Netherlands
(Received 10 February 1993; revised manuscript received 25 May 1993)

A model is put forward, which gives both the intensity and the spectrum of faint light emitted by hot electrons. The model follows from the application of the classical concept of radiation from accelerated charges to electron-phonon collisions. A comparison between the model and the experiment is made for hot electrons in *p-i-n* cold cathodes. The expression for the radiation emitted by a single electron-phonon collision is included in a Monte Carlo calculation of the energy distribution of the electrons. It is found that both the theoretical spectrum and intensity of the emitted radiation are in fair agreement with experiment. The shape of the spectrum is mainly determined by the distribution function of the hot electrons, but the two are not identical. It is found that the intensity of the emitted light scales with the current through the *p-i-n* emitter over several orders of magnitude.

I. INTRODUCTION

In recent years, light-emission microscopy has become an important tool for the failure analysis of integrated circuits (IC's).[1–4] Its value derives from its ability to measure the location of light emission in the interior of an IC. For a long time its use was rather limited due to the very low light levels emitted by IC's, but the introduction of powerful image intensifiers has greatly broadened the area of applications. It has been shown that not only the location of light emission, but also its time dependence and spectral content, provide useful information. In almost all cases, energetic (hot) electrons are responsible for the phenomenon of light emission, but at present the nature of the light-emission process is not completely clear[2,4–9] (bremsstrahlung, interband transitions, recombination). Further insight into the behavior of the IC under test can be obtained from a better understanding of the light-emission mechanisms. In this paper the classical concept of electromagnetic radiation emitted by an accelerated charge (bremsstrahlung) is applied to electron-phonon collisions. This concept is dealt with in detail in Sec. II and the Appendix. *p-i-n* cold cathodes constitute an ideal test system for light emission, because the *n* layer is much thinner than the wavelength, so that interference effects can be neglected. Also, the fairly uniform electric field across the *i* layer gives rise to an energy distribution of hot electrons which is fairly uniform across the *i* layer. Experimental details are given in Sec. III. In Sec. IV the experimental results are presented and discussed within the framework of the theory outlined in this paper. The main conclusions are stated in Sec. V.

II. THEORY

A. The emitted spectrum of one scattering event

Consider a nearly free electron with velocity $\mathbf{v}_i$ and energy E_e (measured from the bottom of the conduction band). Such an electron has a finite probability to emit photons. This probability is determined by the (nonradiative) collisions through which the electron loses its energy. It is clear that only a quantum field theory of the second-order electron-phonon-photon interaction (when the electron loses its energy mainly to phonons) can lead to a correct expression for the spectrum and its intensity. However, here we propose the following expression for the radiative spectrum, based on a semiclassical approach:

$$Q(E_e,\Delta v,\nu)=\frac{e^2\epsilon_r^{1/2}}{3c^3\pi\epsilon_0}\Delta v^2 \quad \text{for } h\nu\le E_e \ , \tag{1}$$

and zero otherwise. $Q(E_e,\Delta v,\nu)d\nu$ is the electromagnetic energy emitted in the frequency range $(\nu,\nu+d\nu)$ by an electron of energy E_e, which undergoes a velocity change Δv in one scattering event; e is the magnitude of the electron charge; ϵ_r is the relative dielectric constant of the material in which emission takes place; c is the speed of light; and ϵ_0 is the permittivity of vacuum. Δv is the magnitude of the change in electron velocity caused by the collision and defined by

$$\Delta v \equiv |\mathbf{v}_f-\mathbf{v}_i| \ , \tag{2}$$

where $\mathbf{v}_f$ is the electron velocity after the collision. The semiclassical treatment, which is described in the Appendix, is based on the assumption that radiative emission from accelerated charges (see Ref. 10) can be applied to the charge acceleration, for example, in electron-phonon collisions. Equation (1) gives a general expression for the magnitude and the shape of the spectrum emitted by an energetic electron in a solid. The cutoff in $Q(E_e,\Delta v,\nu)$ arises from the fact that for photon energies above $\nu_{\max}$ ($\nu_{\max}=E_e/h$, where h is Planck's constant) there are no available end states for the electron (this is a quantum-mechanical argument considering a collision process involving a photon). When $\nu_{\max}$ is approached, the number of available end states decreases because the electron after the collision will be close to the minimum of the conduction band. It is no longer correct to use Eq. (1) for photon emission by such processes, because the density of

states should enter the spectrum [in fact, it does so in Eq. (1), but in a very crude way]. It is therefore expected that close to $\nu_{\max}$ the spectrum will deviate from the form proposed in Eq. (1) by a factor such as $D(E_e-h\nu)/D(E_e)$, where $D(E_e)$ is the electron density of states. In the remainder of this paper we assume that the predominant scattering process is the electron-phonon interaction.

At the least, Eq. (1) is expected to yield reasonable results when the time between collisions is greater than, but still of the order of, the duration of a collision. For Si this holds when $E_e \gtrsim 0.5$ eV. Here reasonable means that the spectrum is of the right order of magnitude and that its shape is fairly constant (at least within a factor of 2). The actual spectra are an average of Eq. (1) over many collisions and different electron energies and their shape is more determined by the energy distribution of electrons $n(E_e)$, than by small variations in the shape of $Q(E_e,\Delta v,\nu)$. Larger deviations in the shape of $Q(E_e,\Delta v,\nu)$ can be expected for photon frequencies close to $\nu_{\max}$ because the density of states starts to play a role. However, as is shown in later calculations, inclusion of the factor $D(E_e-h\nu)/D(E_e)$ has a minimal influence for the spectral range considered in this paper.

For low photon frequencies the validity of Eq. (1) can be questioned when its magnitude becomes comparable with the intensity of a blackbody at the lattice temperature. This is because it is assumed that the photons, once produced by the electrons, have no further interaction with their environment other than by absorption. It will be shown in Sec. II B that, depending on the experimental conditions, the intensity derived from Eq. (1) becomes comparable with the intensity of a blackbody at 400 K for photon energies between 0.4 and 0.8 eV. Also, recombination radiation at the gap energy (for semiconductors) can be much larger than the contribution of Eq. (1). Therefore it is expected that, in the case of Si, Eq. (1) gives a proper description for photon energies above the band gap. Around and below this energy the actual spectrum can be higher due to contributions which are not considered in this paper.

Integrating Eq. (1) gives, for the radiated energy,

$$E_{\text{rad}}=\frac{e^2\epsilon_r^{1/2}}{3c^3\pi\epsilon_0}\Delta v^2\frac{E_e}{h} . \tag{3}$$

In subsequent Monte Carlo calculations, electrons are followed along their path and the radiated energy and the spectrum are determined by summing up contributions according to Eqs. (1) and (3) for each phonon collision taking place. Impact ionization collisions are included in the Monte Carlo simulation, but they are not considered for the light emission because their occurrence is relatively rare. Subsequent phonon collisions of electrons generated in the impact ionization are included in the light-emission calculations.

Between collisions the electrons are continuously being accelerated by the electric field. It is calculated that for a *p-i-n* device the acceleration produced by a field of 10^8 V/m gives at least a factor of 1000 less radiation than the amount produced by the acceleration due to electron-phonon collisions. It is therefore safe not to include the contribution of the electric field.

Summarizing, Eqs. (1) and (3) are to be considered as the minimum amount of radiated energy. From the derivation presented in the Appendix it is to be expected that light emission is a quite general phenomenon when hot electrons are present.

B. Estimate of the spectrum and the emitted power

The following estimates serve to show that hot electrons emit an easily detectable amount of power, much larger than a comparable blackbody, which is proportional to the electrical current, whereas the spectrum is mainly determined by $n(E_e)$, provided that $n(E_e)$ shows a stronger dependence on E_e than the other quantities appearing in the integral of Eq. (9). To evaluate Δv, the following expression is used:

$$\Delta v^2=v_i^2+v_f^2+2v_iv_f\cos\phi , \tag{4}$$

where v_i and v_f are the magnitudes of $\mathbf{v}_i$ and $\mathbf{v}_f$, and ϕ is the angle between these two. Averaging this expression by assuming that all values for ϕ are equally probable, and that for E_e larger than 1 eV v_i and v_f are about equal, yields

$$\overline{\Delta v^2}=2v_i^2 . \tag{5}$$

Here an overlined quantity indicates an average. For an energetic electron in Si, the velocity is estimated by the usual nonparabolic band approximation

$$v_i^2=\frac{2E_e(1+\alpha E_e)}{(1+2\alpha E_e)^2}\frac{1}{m^*} \quad \text{with } \alpha=0.5\ \text{eV}^{-1} , \tag{6}$$

where m^* is the effective electron mass. For $E_e \gtrsim 1$ eV the term in front of $1/m^*$ on the right-hand side of Eq. (6) approaches 1 eV and the estimate for the velocity of an energetic electron becomes

$$v_i^2=\frac{1}{2\alpha m^*}\approx 1.76\times 10^{11}\ \text{m}^2/\text{s}^2 , \tag{7}$$

where for m^* the free-electron mass is substituted. Combining Eqs. (3), (5), and (7) gives

$$\overline{E_{\text{rad}}}\simeq 0.6\times 10^{-8}E_e\epsilon_r^{1/2} . \tag{8}$$

This is the average energy an electron emits when it emits or absorbs an optical phonon. As expected, only a very small fraction of the energy is radiated. It is important to note that this energy is not simply emitted as low-energy photons. According to the spectrum given by Eq. (1), there is a definite possibility that photons with an energy up to E_e are emitted. However, at higher photon energy their number decreases, since the total energy in each frequency interval remains constant. Integrating the number of photons [this is $Q(E_e,\Delta v,\nu)$ divided by $h\nu$] from 1 eV upwards and taking $E_e=2.5$ eV and $\epsilon_r^{1/2}=4$ gives 2.3×10^{-8} for the number of emitted photons in the corresponding frequency interval. So one out of 4.3×10^7 phonon collisions gives rise to the emission of a photon with an energy between 1 and 2.5 eV.

In a *p-i-n* device carrying an electric current I_{el} there are electrons of different energies, and each electron experiences many collisions while traversing the device. Integrating over all collisions gives, for the intensity of the spectrum,

$$I(\nu)=\frac{e^2V}{3c^3\pi\epsilon_0}\int_{h\nu}^{\infty}\frac{\epsilon_r^{1/2}\Delta v^2 n(E_e)v_e(E_e)}{\lambda_{\text{el-ph}}(E_e)}dE_e \ . \quad (9)$$

V is the volume of the *p-i-n* emitter having an active length l. Assuming that Δv, ϵ_r, v_e, and $\lambda_{\text{el-ph}}$ have a much weaker energy dependence than $n(E_e)$, the above expression reduces to

$$I(\nu)=\left[\frac{e^2\overline{\Delta v^2}\,\overline{\epsilon_r^{1/2}}}{3c^3\pi\epsilon_0}\right]\left[\frac{lI_{el}}{\lambda_{\text{el-ph}}e}\right]\frac{\int_{h\nu}^{\infty}n(E_e)dE}{\int_0^{\infty}n(E_e)dE} \ . \quad (10)$$

Here the first term on the right-hand side is the average "strength" of the spectrum emitted in one collision, the second term is the number of collisions per second (equal to the number of collisions per electron times the number of electrons per second), and the last term determines the shape of the spectrum. The emitted power is obtained by integrating the spectrum:

$$W=2.3\times10^{-8}\frac{l}{\lambda_{\text{el-ph}}}\frac{I_{el}}{e}\overline{E_e} \ . \quad (11)$$

Here we used the previous estimate for $\overline{\Delta v^2}$ and $\overline{\epsilon_r^{1/2}}=4$. This expression can simply be interpreted as the number of collisions times the average energy emitted in one collision. Entering numbers applicable to the *p-i-n* devices, $l=50$ nm, $\overline{\lambda_{\text{el-ph}}}=1$ nm, and $\overline{E_e}=1.3$ eV, gives

$$\overline{W}=a_0I_{el} \quad \text{with } a_0=1.55\times10^{-6}\ \text{W/A} \ . \quad (12)$$

$\overline{E_e}$ is determined from the energy distribution of hot electrons calculated with the Monte Carlo code for an applied voltage of 7 V on the *p-i-n* device.

To make an order-of-magnitude comparison with blackbody radiation, we assume for the moment that the power given by Eq. (12) is emitted as a spectrum with constant intensity up to 1 eV. Then the value of this intensity has the same numerical value given by Eq. (12). The electrical currents used in the *p-i-n* device are between 10^{-3} and 10^{-7} A. The intensities calculated for these currents are compared with a blackbody at 400 K with an area of 10^{-10} m^2 (the upper limit of the *p-i-n* device). It is found that the two have equal intensity at 0.4 eV (for 10^{-3} A) and 0.75 eV (for 10^{-7} A). Since the intensity of the blackbody falls so rapidly with increasing frequency, it can be concluded that above 1.0 eV the spectrum of a *p-i-n* device is several orders of magnitude larger than the spectrum of a blackbody at a (an already increased) temperature of 400 K.

C. The detected radiation

When radiation is generated inside a medium, and the detector is in another medium, only radiation lying within a cone determined by the critical angle will be able to cross the interface. The intensity is further reduced by the numerical aperture (NA) of the detector, reflection at the interface, and absorption. When the medium of the detector is air, the following spectrum will be detected:[11]

$$I_d(\nu)=\frac{2n}{(n+1)^2}[1-\cos(\theta_c)]\exp\left[-\frac{4\pi kd}{\lambda}\right]I_e(\nu) \ . \quad (13)$$

Here it is assumed that a point source in the medium emits isotropic radiation $I_e(\nu)$. The spectrum arriving at the detector is denoted by $I_d(\nu)$, n is the (frequency-dependent) refractive index, k is the imaginary part of the square root of the dielectric constant, d is the length to be traveled to reach the interface, and θ_c is the solid cone inside the medium that reaches the detector:

$$\theta_c=\arcsin NA/n \ . \quad (14)$$

For the case of NA equal to 1, θ_c is equal to the critical angle. The first term on the right-hand side of Eq. (13) is the transmission at normal incidence divided by 2. For Si the refractive index is rather large and therefore the transmission remains approximately constant up to the critical angle. The solid cone is responsible for the factor of 2 and the second term, whereas the third term accounts for absorption. Because θ_c is rather small for Si, the distance to the interface has been approximated by the same value for all light rays. Since the refractive index depends on photon frequency, Eq. (13) implies both a distortion of the spectrum and a considerable reduction in intensity. Comparing the spectra for different NA's in the range 0.2–0.8, it is found that detected intensities change, but the shape of the spectra is not noticeably affected. It is pointed out that in most work on photon emission by hot electrons the effects of Eq. (13) are neglected.

III. SIMULATION AND EXPERIMENTAL DETAILS

A. The Monte Carlo code

The computer simulation is performed with a slightly adapted version of the Monte Carlo code developed by Tang and Hess.[12] The electrons, which move in the silicon band structure, are subject to an external electric field, to phonon scattering, and to impact ionization. For each value of the external electric field the motion of 3000 electrons is calculated. More details can be found in Refs. 12–14.

B. Spectra

The experimental setup shown in Fig. 1 is used for measuring the spectrum of light emitted by the DUT (device under test). The sidearm starting with the prism is mounted on a modulo pack of a Leitz microscope. The movable mirror is mounted inside the modulo pack, where it can be moved in the optical path to divert the optical beam to the sidearm. This setup is described more fully in Ref. 15. A spectrum manifests itself as a bright line on the image intensifier, where each pixel corresponds to a certain wavelength. The gain of the image intensifier is variable between approximately 70 000 and 700 000, and cooling is employed to reduce the noise of

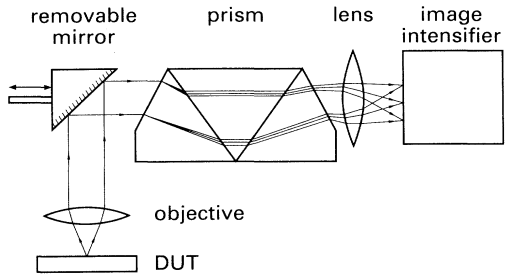

FIG. 1. The experimental setup including microscope and sidearm, which contains prism, lens, and image intensifier.

the image intensifier. Before starting a measurement, a narrow-band optical filter is used to position the microscope in such a way that the transmitted wavelength arrives at the corresponding pixel. This is important, since any angular deviation of the beam entering the prism results in a shift of the spectrum. Also, the prism can be moved in and out of the light path in order to check the direction of the incoming beam.

A measurement is done by averaging the picture on the image intensifier with a computer-controlled image processor. In the same manner a background picture is taken with the optical source switched off. After subtracting the background the image is converted into a spectrum. This involves calibration tables including, for example, the prism properties and the spectral sensitivity of the image intensifier. The latter mainly determines the spectral range of 400 (3.15 eV) to 900 nm (1.40 eV) covered by this setup. The calibration tables have been obtained by measuring the calibrated spectrum of a halogen lamp and by measuring a blackbody radiator at 773 K. The absolute intensity scale was derived from the total emission of a *p-i-n* device measured with a photodiode placed directly on top of it. The dependence of the gain of the image intensifier on control voltage was measured separately. It is estimated that these calibration procedures give an absolute intensity which is accurate within a factor of 2.

C. *p-i-n* cold cathode

The cold cathodes used here are Si devices consisting of a B-doped *p* layer, a 45-nm intrinsic (*i*) layer and a top layer 10 nm thick. The inset in Fig. 2 displays a cross section of the device; more details can be found elsewhere.[16] The *I-V* characteristic in Fig. 2 shows the onset of breakdown at a reverse bias of approximately 6.5 V, giving rise to a strong current increase. All measurements are performed with the *p-i-n* devices at room temperature and negative (reverse) bias voltage.

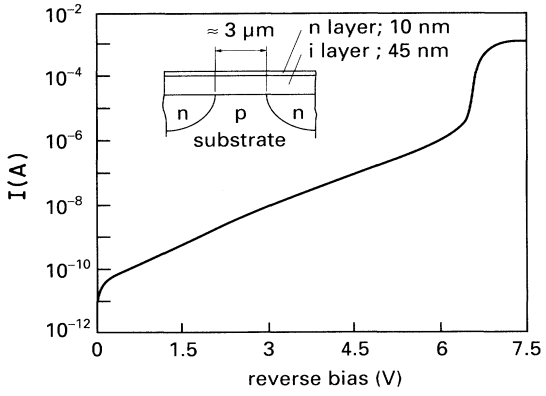

FIG. 2. *I-V* characteristic of a *p-i-n* cold cathode for reverse bias. The inset shows a cross section of the device.

IV. RESULTS AND DISCUSSION

A. Shape of the spectra

In Fig. 3 measurements at different voltages are compared with theoretical calculations. In the Monte Carlo code the contribution of each collision to the spectrum is summed up. Subsequently Eq. (13), with the omission of the absorption term, is used to calculate the spectrum in air. Both calculations and measurements are normalized at 2 eV. It can be seen that there is good agreement between theory and experiment. At 7 and 4 V two sets of theoretical curves appear; one is calculated as described earlier and in the other the term containing the density of states [as was suggested in the text preceding Eq. (3)] is included. At 7 V this gives a slightly better agreement for photon energies above 2.6 eV. At 4 V there is no significant difference between the two theories at the higher photon energies. At 4 V the intensity of the emitted light is very low, resulting in a higher noise level. When the spectra at different voltages are compared it is observed that they only show small differences, both experimentally and theoretically. This is shown in Fig. 4.

Figure 5 stresses the importance of including Eq. (13) (without absorption term). Calculations performed for 7 V are shown, one curve includes Eq. (13) (labeled in air), the other omits it (labeled in Si). The shapes of the two spectra differ significantly, leading to an intensity difference of more than a factor 2 at 3 eV. In comparison, including absorption leads to a decrease of only 17% at 3 eV, and this results in a minor change in the shape of the spectrum as is exemplified by the curve labeled "with k." Also, the inclusion of the density of states results in a minor change, but of opposite sign, giving an increase of around 30% at 3 eV. In subsequent calculations we will omit the effects of absorption and density of states.

The theory of Sec. II suggests that the shape of the spectra is related to the energy distribution function of the electrons. If the simplifications made in arriving at Eq. (10) are justified, then the spectrum is proportional to $\int_{h\nu}^{\infty} n(E_e)dE$, whereas in other work on hot electrons[2,17] it is often assumed that the spectra have the same shape as $n(E_e)$. In Fig. 6 the calculated spectrum in Si is compared with calculations of $n(E_e)$ and $\int_{h\nu}^{\infty} n(E_e)dE$, all of which are performed for a reverse bias of 7 V. It can be seen that the spectrum and the quantities involving $n(E_e)$ all have a different shape. $n(E_e)$ and its integral are quite similar above 1.75 eV. Below 2.1 eV the calculated spectrum coincides with $\int_{h\nu}^{\infty} n(E_e)dE$, but above 2.1 eV the calculated spectrum in Si decreases more rapidly. As was shown earlier, the calculated spectrum in air decreases even more rapidly. The same behavior is

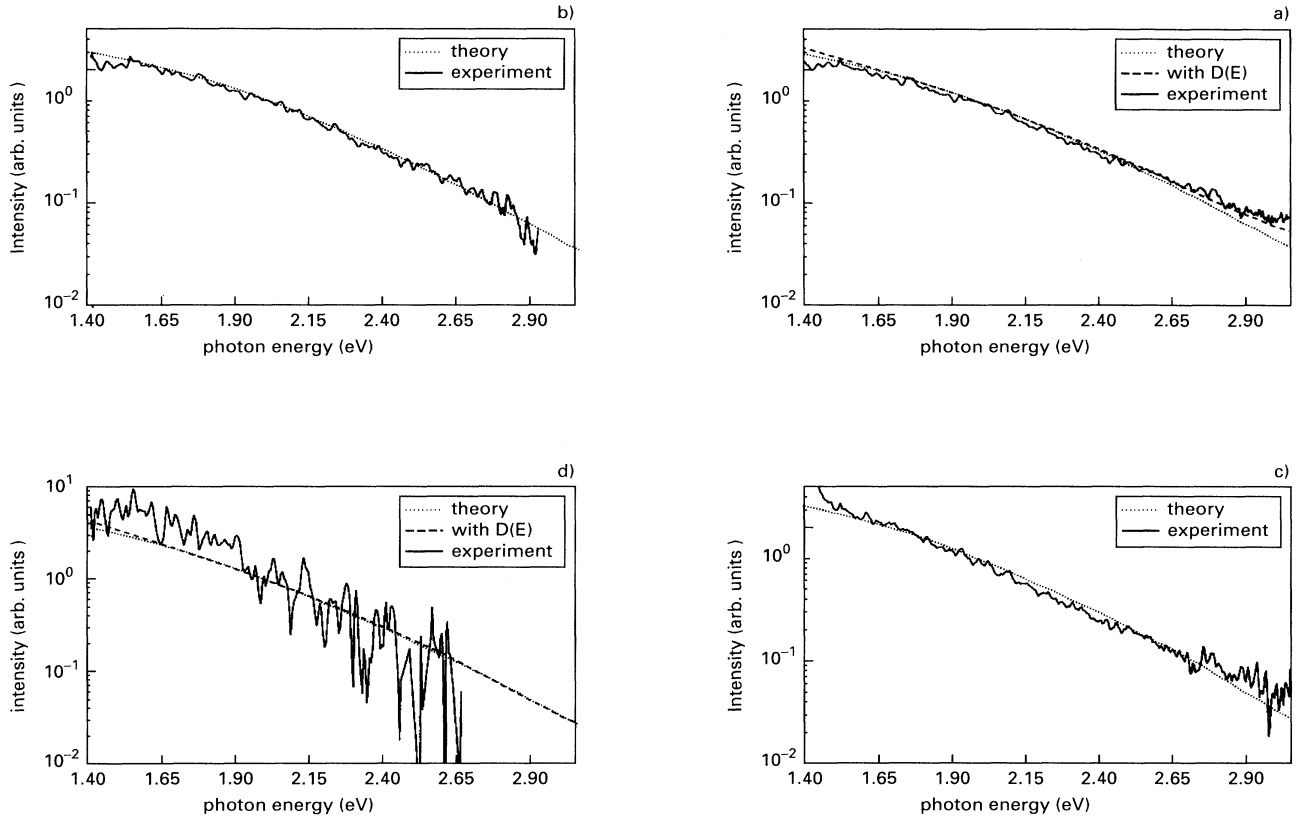

FIG. 3. Measured and calculated spectra normalized at 2 eV. (a) Reverse bias of 7 V, (b) reverse bias of 6 V, (c) reverse bias of 5 V, and (d) reverse bias of 4 V. In (a) and (d) a calculation incorporating the effect of the density of states $D(E)$ is also displayed.

found for other bias voltages. It is concluded that for the spectral range shown in Fig. 6 the shape of the measured spectrum corresponds neither with $n(E_e)$ nor with its integral. This invalidates the frequently made conjecture about the relation between spectra and $n(E_e)$ made in the literature. The estimate in Sec. II C is also too coarse for an accurate description of the spectrum (in Si). It is somewhat surprising that the discrepancy occurs at the highest photon energies, where $n(E_e)$ shows the strongest decrease, since here the assumption that $n(E_e)$ shows a stronger dependence on photon energy than the other quantities in Eq. (9) seems most easily be fulfilled. The implication of these findings is that if a temperature is derived from the high-frequency tail of the measured spectra, it is bound to be too low when compared with a temperature derived from the high-frequency tail of $n(E_e)$. This is caused by the difference in shape between the calculated spectrum (in Si) and the electron density on the one hand, and the deformation of the spectrum when it is emitted from Si into air on the other. One of us (H.B.) reported about the inadequacy of the temperature concept for hot electrons.[18]

B. Absolute intensities

The absolute intensities of the spectra are plotted in Fig. 7, where they are compared with theoretical calculations obtained by multiplying the theoretical data by the measured current. No fit parameters are used. The measured intensities are larger than the theoretical curves (in air), but the difference becomes smaller for lower voltages (and currents). Below the breakdown voltage leakage currents exist, which probably do not give rise to the same type of light emission as discussed here. Therefore, the currents used to multiply the calculated spectra can be too large at the lowest current levels, which could make the better correspondence between intensities at lower voltages fortuitous. In any case, the agreement between intensity levels is within an order of magnitude, which is not unreasonable in view of the assumptions made in the derivation of Eq. (1). It is clear from Fig. 7 that the intensity measured in air is two orders of magnitude less than the one generated in Si, and the measured intensities are always in between. Although the emission of one particular collision event has a maximum emission probability in a direction perpendicular to Δv (according to classical electrodynamics), the directions of Δv show a random distribution. Therefore, the emitted radiation inside Si is not expected to show a particular direction preference, leading to a larger intensity emitted in air.

Figure 8 displays a double logarithmic plot of the total intensity in the range 1.4–3.05 eV against the electrical current. The theoretical intensities are obtained by integrating the theoretical spectra over the same energy range. Theory predicts a linear relation between current

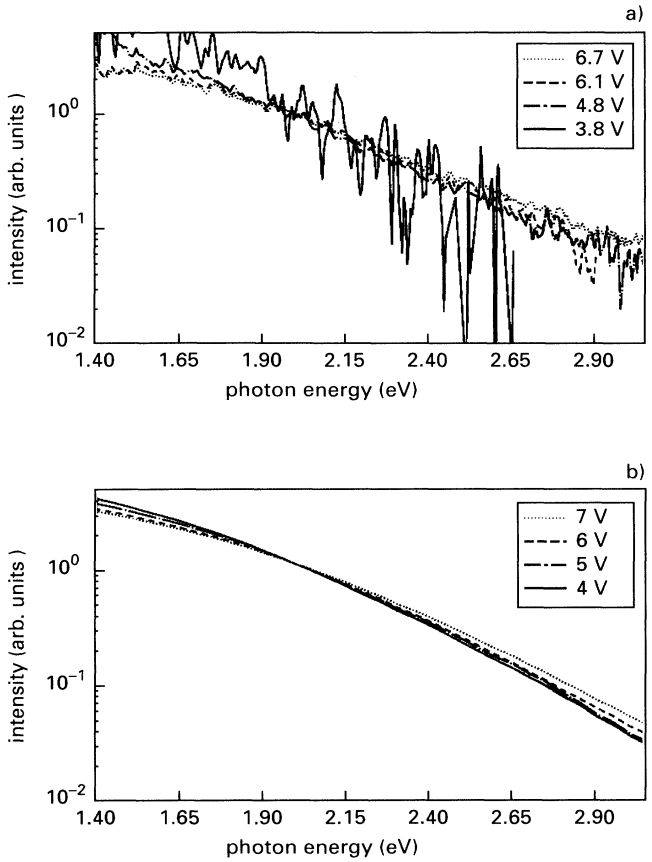

FIG. 4. Comparison of spectra: (a) experimental spectra; and (b) theoretical spectra.

and emitted power [Eq. (12)], and this is confirmed by the theoretical curve (which is based on the Monte Carlo calculations). In contrast, the experimental curve at the higher currents is fitted by

$$W = 5.8 \times 10^{-8} I_{\mathrm{el}}^{0.88} \ . \tag{15}$$

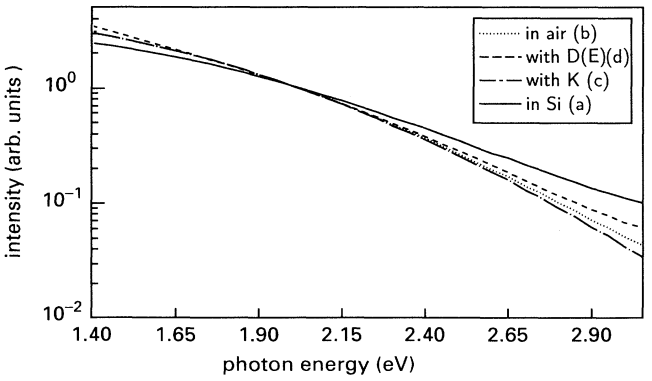

FIG. 5. Calculated spectra for 7 V reverse bias showing the effect of various approximations: (a) spectrum within the medium; (b) spectrum in air, no absorption; (c) spectrum in air, including absorption; and (d) spectrum in air, including density of states.

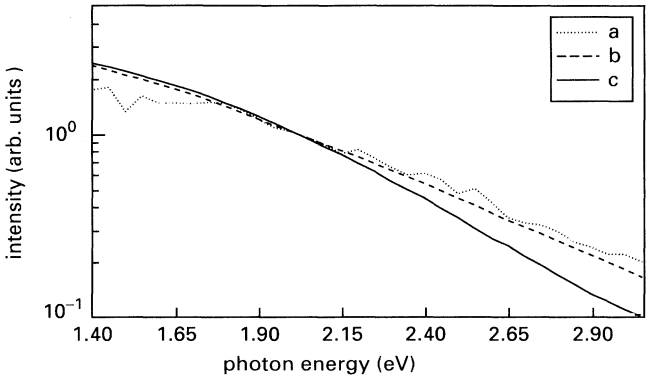

FIG. 6. Comparison at 7 V reverse bias between the electron energy distribution $n(E)$ and the calculated spectrum inside Si: (*a*) $n(E)$; (*b*) Int($n(E)$); and (*c*) calculated spectrum inside Si.

This discrepancy cannot be explained by leakage currents, since these are only apparent at low currents. As the theoretical results show, the small change in the shape of spectra does not cause a change in linearity. Also, it is observed that different samples show the same behavior at higher currents, whereas the differences at low currents can be ascribed to leakage currents. Effects of series resistance and power dissipation are expected to increase rapidly at the highest currents and are therefore not good candidates to explain the observed behavior. At the moment we fail to understand the discrepancy at higher currents. Tentative explanations are effects of mutual interactions of electrons (e.g., space-charge effects), which are disregarded in the model, or systematic deviations in the experimental determination of the intensities.

V. CONCLUSIONS

The spectra of light emitted by reverse-biased *p-i-n* devices have been measured for different bias conditions. The shape of the spectra is accurately described by a model based on the classical bremsstrahlung concept applied to electrons interacting with optical phonons. Within an order of magnitude this model also explains the intensity of the emitted light. When light is detected outside the device, not only is its intensity reduced by two orders of magnitude, but the spectrum also changes shape. The shape of the spectra does not coincide with the energy distribution function of hot electrons. The model developed here can be applied equally well to other devices where hot electrons come into play.

Note added in proof. Recently two references have come to our attention which are relevant to this paper. The first reference of Lacaita *et al.*[19] critically discusses the concept of bremsstrahlung as treated by Figielski and Torun. We want to remark that our treatment of bremsstrahlung accounts for the discrepancies noted by Lacaita *et al.*: it gives the right order of magnitude for the intensity; it is not dependent on impurity concentration and it shows no temperature dependence. The treatment of Bude, Sano, and Yoshii[20] is the quantum-mechanical version of our approach for the indirect phonon-assisted

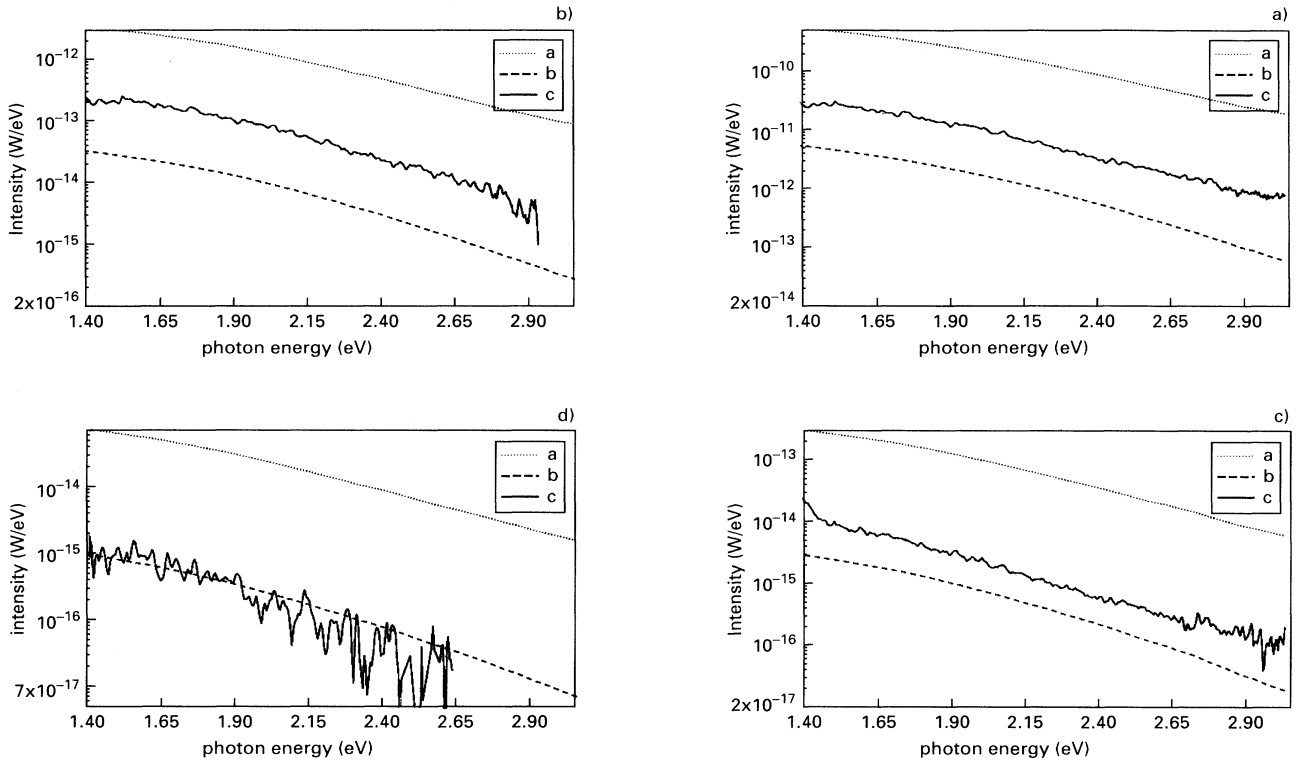

FIG. 7. Absolute intensities of calculated spectra inside Si (*a*), outside Si (*b*), and of measured spectra (*c*). Reverse bias of 7 (a), 6 (b), 5 (c), and 4 V (d).

conduction-band to conduction-band transitions. No easy comparison is possible at the moment since the "electron temperature" in the *p-i-n* devices is considerably higher (7000 K) than in the cases considered by Bude, Sano, and Yoshii.[20]

ACKNOWLEDGMENTS

We would like to thank Tom van Zutphen for many useful discussions on the subject of *p-i-n* devices. He and Bert Lindelauf kindly supplied us with samples. The Monte Carlo code used here is an adapted version of the code developed by Tang and Hess, which was kindly presented to us. We would like to thank K. Hess, J. Higman, and D. Arnold for fruitful discussions. Part of this work was carried out within the Jessi T4C project.

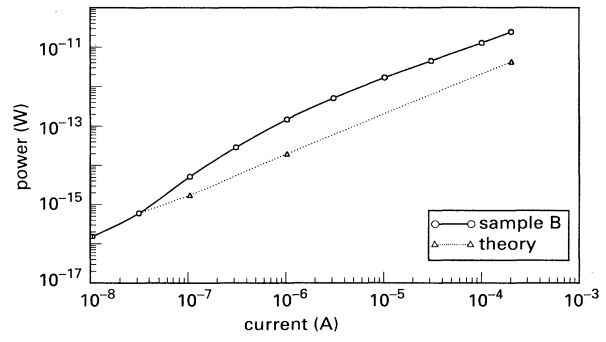

FIG. 8. The emitted power in the range from 1.4 to 3.15 eV as a function of the electrical current through the *p-i-n* cold cathode. Theoretical points are calculated using the calculated spectra (labeled *b*) in Fig. 7.

APPENDIX

Here we want to justify Eq. (1). There are two ways to proceed: one is to consider all possible collision processes in which photon emission is allowed and calculate the transition probabilities by evaluating the proper matrix elements according to quantum mechanics; the other is a classical approach in which the acceleration **a** (due to collision processes) of the electron is used to determine the radiated energy. According to the correspondence principle, the two approaches should yield the same results for high electron energy. The classical approach was used by Kramers[10] for the calculation of the continuous x-ray spectrum, and by Figielski and Torun[6] to calculate light emission from hot electrons scattered by charged impurities. In both cases the mechanism for light emission is the acceleration of the electron charge. Here too, we will follow the classical approach, but unlike Figielski and Torun the acceleration **a** will be determined from the predominant scattering process. Classical electrodynamics predicts that a nonrelativistic electron subject to an acceleration **a** emits radiation at a rate of

$$\frac{dE}{dt} = \frac{e^2}{6c^3\pi\epsilon_0} a^2 \epsilon_r^{1/2} , \tag{A1}$$

where a is the magnitude of **a**, E is the energy of the emitted radiation, and ϵ_r is the relative dielectric constant of the medium in which the emission takes place. In order

to determine the spectrum, **a** has to be known. We start with an ansatz for the acceleration of an electron during a collision, and from the calculated spectrum for this specific case an educated guess is made for the spectrum in the general case, where the specific choice of the ansatz will no longer play a role. The ansatz is that the direction of **a** is constant and that its magnitude is given by

$$a(t)=a_0 \text{ for } -0.5\tau_d \le t \le 0.5\tau_d \tag{A2}$$

and $a(t)=0$ otherwise. Here τ_d is the duration of the collision. Substituting this into Eq. (A1) and integration over time yields the total amount of radiated energy:

$$E_{\text{rad}}=\frac{e^2}{6c^3\pi\epsilon_0}\epsilon_r^{1/2}a_0^2\tau_d \ . \tag{A3}$$

To find the frequency components in Eq. (A1), the Fourier transform $A(\nu)$ of $a(t)$ is used in a manner similar to Kramers.[10] A direct calculation gives

$$A(\nu)=\Delta v\frac{\sin(\pi\tau_d\nu)}{\pi\tau_d\nu} \ , \tag{A4}$$

and the velocity change Δv is given by

$$\Delta v=a_0\tau_d \ . \tag{A5}$$

It is important to note that the velocity change can be different from zero, even if the magnitudes of the velocities before and after the collision are equal.

We now use Parceval's theorem

$$\int_{-\infty}^{\infty}a^2(t)dt=2\int_0^{\infty}|A^2(\nu)|d\nu \tag{A6}$$

to obtain an expression for E_{rad} in terms of an integral over ν. Also, E_{rad} can be found by integrating the spectrum, yielding the following equality:

$$\frac{2e^2}{6c^3\pi\epsilon_0}\epsilon_r^{1/2}\int_0^{\infty}|A^2(\nu)|d\nu=\int_0^{\infty}Q(E_e,\nu)d\nu \ . \tag{A7}$$

Evocating the correspondence principle in a manner similar to Kramers,[10] the solution

$$Q(E_e,\nu)=\frac{e^2}{3c^3\pi\epsilon_0}\epsilon_r^{1/2}|A^2(\nu)| \tag{A8}$$

is interpreted as the emitted spectrum. Substituting the expression for $A(\nu)$ gives

$$Q(E_e,\Delta v,\nu)=\frac{e^2\epsilon_r^{1/2}}{3c^3\pi\epsilon_0}\Delta v^2\frac{\sin^2(\pi\tau_d\nu)}{(\pi\tau_d\nu)^2} \ . \tag{A9}$$

Now an estimate for τ_d will be made. During the collision the energy of the electron is not well defined and the maximum uncertainty is E_e. Using the uncertainty relation for time and energy, the minimum collision duration can be estimated as

$$E_e\tau_d=\hbar \ . \tag{A10}$$

The maximum collision duration is determined by τ_c, the time between collisions. Assuming that (on the average) between collisions an electron gains an amount of energy equal to the amount it loses by the collision, it is found that

$$eE\tau_c v_i=\overline{E_{\text{ph}}}\approx 8\times 10^{-21}\ \text{J} \ . \tag{A11}$$

Here E is the electric field, and in the approximation we used a phonon energy of 0.05 eV. Substitution of $E=10^8$ V/m and the value derived in Sec. II for the electron velocity of energetic electrons gives

$$\tau_c\approx 1.2\times 10^{-15}\ \text{s} \ . \tag{A12}$$

At $E_e=1$ eV, τ_c is a factor of 2 larger than τ_d. Therefore, at the least Eq. (A10) is considered to give the correct order of magnitude when $E_e\gtrsim 0.5$ eV. Another estimate of the collision time is found by taking the time an electron needs to travel one wavelength (determined by its wave vector). Apart from a factor π, this gives the same result as Eq. (A10), but the whole concept of a definite wave vector for a particle experiencing collisions within a few wavelengths becomes questionable, and the wave vector may no longer be a good quantum number. Therefore, the energy argument used above is at present the best one we can come up with. Using Eqs. (A9) and (A10), the spectrum becomes

$$Q(E_e,\Delta v,\nu)=\left[\frac{e^2\epsilon_r^{1/2}}{3c^3\pi\epsilon_0}\Delta v^2\right]\frac{\sin^2\left[\frac{h\nu}{2E_e}\right]}{\left[\frac{h\nu}{2E_e}\right]^2} \ . \tag{A13}$$

Energy conservation requires that the maximum photon frequency $\nu_{\max}$ equals E_e/h. For frequencies far below $\nu_{\max}$ the spectrum is determined by the prefactor [the first term in parentheses on the right-hand side of Eq. (A13)], but close to $\nu_{\max}$ the second term (involving the sine) comes into play and it reaches a value of 0.91 at $\nu_{\max}$. Here the estimate of Eq. (A10) determines the value at $\nu_{\max}$.

The small decrease of the spectrum toward $\nu_{\max}$ arises from the ansatz for the time dependence of a. If the square were replaced by a Gaussian or a Lorentzian, the amplitude towards $\nu_{\max}$ shows some decrease, but as long as we request that $a(t)$ vanishes for times larger than τ_d, this decrease is fairly small: for $a(t)=a_0\exp(-t/\tau_d)^2$, it is 0.61, and for $a(t)=a_0/[1+(2\pi t/\tau_d)]^2$ it amounts to 0.73.

Here we will make the generalization that the prefactor contains the essential physics and we therefore postulate the following spectrum:

$$Q(E_e,\Delta v,\nu)=\frac{e^2\epsilon_r^{1/2}}{3c^3\pi\epsilon_0}\Delta v^2 \text{ for } h\nu\le E_e \tag{A14}$$

and $Q(E_e,\Delta v,\nu)=0$ otherwise. When Eq. (A14) is integrated, the emitted energy becomes

$$E_{\text{rad}}=\frac{e^2\epsilon_r^{1/2}}{3c^3\pi\epsilon_0}\Delta v^2\frac{E_e}{h} \ . \tag{A15}$$

This expression is a factor 0.34 less than the amount calculated from Eqs. (A3) and (A10) because the spectrum is truncated at $\nu_{\max}$. Again, the difference depends on the specific ansatz for $a(t)$, but they all yield a factor of the same magnitude (between 0.34 and 1). Therefore, the total emitted energy given by Eq. (A15) is of the right order of magnitude.

[1]N. Khurana, T. Malone, and W. Yeh, *Proceedings of the 23rd Reliability Physics Symposium, Orlando, FL* (IEEE, New York, 1985), p. 212.

[2]Akira Toriumi, Makoto Yoshimi, Masao Iwase, Yutaka Akiyama, and Kenji Taniguchi, IEEE Trans. Electron Dev. **ED-34**, 1501 (1987).

[3]Siak-Cheiw Lim and Eng-Guan Tan, *Proceedings of the 26th Reliability Physics Symposium, Monterey, CA* (IEEE, New York, 1988), p. 119.

[4]Massimo Lanzoni, M. Manfredi, L. Solmi, Enrico Sangiorgi, R. Capelletti, and Bruno Ricco, IEEE Electron Dev. Lett. **10**, 173 (1989).

[5]A. G. Chynoweth and K. G. McKay, Phys. Rev. **102**, 369 (1956).

[6]T. Figielski and A. Torun, in *Proceedings of the International Conference on the Physics of Semiconductors,* edited by A. Stickland (Institute of Physics, London, 1962), p. 863.

[7]Simon Tam and Chenming Hu, IEEE Trans. Electron Dev. **ED-31**, 1264 (1984).

[8]M. Lanzoni, E. Sangiorgi, C. Fiegna, M. Manfredi, and B. Ricco, *International Electron Devices Meeting 1990* (IEEE, New York, 1990), p. 69.

[9]A. Lacaita, Semicond. Sci. Technol. B **7**, 590 (1992).

[10]H. A. Kramers, Philos. Mag. **46**, 836 (1923).

[11]See, for example, S. M. Sze, *Physics of Semiconductor Devices* (Wiley, New York, 1981), p. 694.

[12]J. Y. Tang and K. Hess, J. Appl. Phys. **54**, 5139 (1983).

[13]J. M. Higman, K. Kim, K. Hess, T. van Zutphen, and H. M. J. Boots, Appl. Phys. Lett. **65**, 1384 (1989).

[14]H. M. J. Boots, M. F. H. Schuurmans, D. Arnold, J. M. Higman, and K. Hess, Appl. Phys. Lett. **57**, 2446 (1990).

[15]Kees de Kort and Paul Damink (unpublished).

[16]P. A. M. van der Heide, G. G. P. van Gorkom, A. M. E. Hoeberechts, A. A. van Gorkum, and G. F. A. van der Walle, in *Proceedings of the Second International Conference on Vacuum Microelectronics 1989,* IOP Conf. Proc. No. 99 (Institute of Physics, Bristol, 1984), p. 141.

[17]Massimo Lanzoni, Enrico Sangiorgi, Claudio Fiegna, Manfredo Manfredi, and Bruno Ricco, IEEE Electron Dev. Lett. **12**, 341 (1991).

[18]H. M. J. Boots, Phys. Rev. B **46**, 9428 (1992).

[19]Andrea L. Lacaita, Franco Zappa, Stefano Bigliardi, and Manfredo Manfredi, IEEE Trans. Electron Dev. **ED-40**, 577 (1993).

[20]Jeff Bude, Nobuyuki Sano, and Akira Yoshii, Phys. Rev. B **45**, 5848 (1992).